Available online at www.sciencedirect.com
SCIENCE DIRECT®
Journal of Sound and Vibration 277 (2004) 801–814
JOURNAL OF SOUND AND VIBRATION
www.elsevier.com/locate/jsvi

Finite element vibration analysis of composite box structures using the high order plate theory

S.-Y. Lee, S.-C. Wooh*

Department of Civil and Environmental Engineering, Massachusetts Institute of Technology, 77 Massachusetts Avenue, Cambridge, MA 02139-4307, USA

Received 13 December 2002; accepted 9 September 2003

Abstract

This study deals with free vibration of folded structures and box beams made of composite materials using a four-noded Lagrangian and Hermite finite element that incorporates high order transverse shear deformation and rotary inertia. An 8×8 matrix is assembled to transform the system element matrices from the local to global co-ordinates, in which an eighth drilling degree of freedom (d.o.f.) per node is appended to the existing 7-d.o.f. system. The results obtained are in good agreement with the semi-analytical solutions and numerical results reported by other investigators. Sample studies are carried out for various layup configurations and boundary conditions. The significance of the high order plate theory in analyzing folded structures is enunciated in this paper.

1. Introduction

Folded plates or box members offer a broad range of structural engineering applications such as culverts, ship hulls, buildings, and box girder bridges. With the advancement of technology in fiber-reinforced composite materials, the applicability of composites to such members has been increased significantly due to their merits such as low density, high stiffnesses and high strengths.

Structural behavior of folded isotropic plates has been studied previously by a host of investigators using a variety of approaches. Goldberg and Leve [1] developed a method based on elasticity, which was subsequently modified and applied by De Fries-Skene and Scordelis [2]. The methods in this category are common because of their superb computational accuracy. However, it is difficult to apply these methods directly to folded plates or to dynamic problems, so that they

*Corresponding author. Tel.: +1-617-253-7134/6044; fax: +1-617-253-6044.
E-mail address: scwooh@mit.edu (S.-C. Wooh).

0022-460X/$ - see front matter
doi:10.1016/j.jsv.2003.09.024

have been extended by other investigators to deal with those problems. For example, Scordelis [3] and Chu and Dudnik [4] analyzed simply supported box bridges using a similar technique. Cheung [5] introduced the finite strip method for analyzing folded prismatic plates and box girders. Liu and Huang [6] solved the problems for one- and two-folded plates using a finite element-transfer matrix method. Zienkiewicz and Taylor [7] presented a flat shell technique which can be applied directly to folded plates. Dynamic problems are also tackled by many investigators. For example, Irie et al. [8] calculated the natural frequencies of folded cantilever plates using the Ritz method. Danial [9] introduced a concept referred to as spectral element method. Lee et al. [10] analyzed the dynamic response of a prestressed concrete box girder bridge subjected to moving loads using folded plate elements.

All these works are limited, in that they can analyze only the structural members made of isotropic materials. Recently, techniques for analyzing anisotropic plates are evolved. Suresh and Malhotra [11] studied the free vibration of damped composite box beams using four-node plate elements with five degrees of freedom (d.o.f.) per node. Niyogi et al. [12] carried out a finite element vibration analysis of folded laminates using a first order plate theory (FOPT). In general, a first order shear deformation theory can describe easily and accurately the kinematic behavior of a flat composite plate [13]. However, it requires an estimation of shear correction factors; a value of $K = \frac{5}{6}$ is normally used [14]. On the other hand, a high order plate theory (HOPT) is free from such requirements and thus can yield more accurate results for both static and dynamic conditions than those of the first order theories. This allows for convenient use of HOPT. Many high order theories exist but they are mostly applicable to unfolded (flat) isotropic or anisotropic plates at the present time [15–18]. In this paper, the existing HOPT are extended to study free vibration of folded and box structures made of composite materials.

2. Theoretical formulation

The HOPT for analyzing unfolded laminates reviewed in this study is derived from the third order laminate formulation of Reddy [13]. To analyze folded anisotropic structures, we introduce a modified displacement finite element model using non-conforming elements of 8-d.o.f. (including the drilling degree of freedom) per node.

2.1. High order plate theory

The HOPT presented in this paper is based on the same assumptions as those of the classical and first order plate theories, except that we no longer assume that the straight lines normal to the middle surface remain straight after deformation but it is assumed that they can be expressed in the form of a cubic equation. Fig. 1 shows schematically the deformation kinematics of the three different models. The displacement field for the HOPT now can be expressed as [13]

$$\begin{aligned} u(x,y,z,t) &= u_0(x,y,t) + z\phi_x(x,y,t) - c_1 z^3(\phi_x + c_0 w_{0,x}),\\ v(x,y,z,t) &= v_0(x,y,t) + z\phi_y(x,y,t) - c_1 z^3(\phi_y + c_0 w_{0,y}),\\ w(x,y,z,t) &= w_0(x,y,z,t), \end{aligned} \tag{1}$$

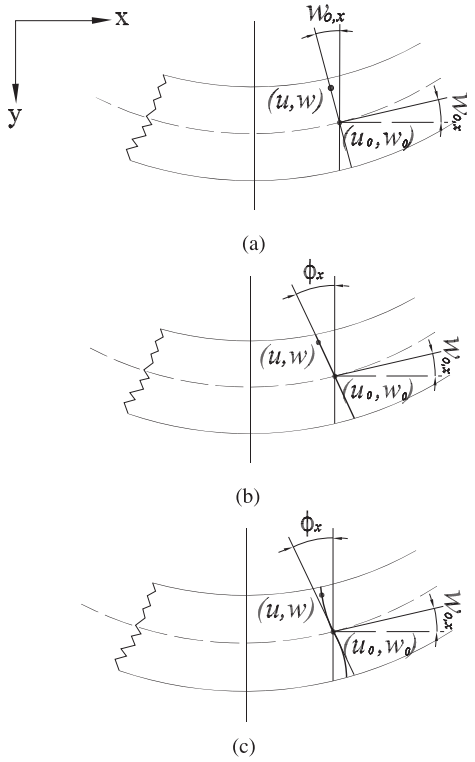

Fig. 1. Assumed deformation of a straight line normal to the middle surface of a plate for (a) classical laminated plate theory (CLPT), (b) first order plate theory (FOPT), and (c) high order plate theory (HOPT).

where u_0, v_0 and w_0 are the mid-plane displacements in the x, y and z directions, ϕ_x and ϕ_y are the rotations, and c_0 and c_1 are the parameters referred to as *tracers*. The condition $c_0 = 1, \phi_x = -w_{0,x}$ and $\phi_y = -w_{0,y}$ in Eq. (1) yields the same displacement field as that of the classical lamination theory (CLPT). The displacement field becomes identical to that of FOPT for $c_1 = 0$. Note that $c_0 = 1$ for HOPT.

The equations of motion for the HOPT are derived using the principle of virtual displacements. The following Euler–Lagrange equations can be obtained using the calculus of variations [13]:

$$\frac{\partial N_{xx}}{\partial x} + \frac{\partial N_{xy}}{\partial y} = I_0\ddot{u}_0 + J_1\ddot{\phi}_x - c_1 I_3 \frac{\partial \ddot{w}_0}{\partial x},$$

$$\frac{\partial N_{xy}}{\partial x} + \frac{\partial N_{yy}}{\partial y} = I_0\ddot{v}_0 + J_1\ddot{\phi}_y - c_1 I_3 \frac{\partial \ddot{w}_0}{\partial y},$$

$$\frac{\partial \bar{Q}_x}{\partial x} + \frac{\partial \bar{Q}_y}{\partial y} + \frac{\partial}{\partial x}\left(N_{xx}\frac{\partial w_0}{\partial x} + N_{xy}\frac{\partial w_0}{\partial y}\right) + \frac{\partial}{\partial y}\left(N_{xy}\frac{\partial w_0}{\partial x} + N_{yy}\frac{\partial w_0}{\partial y}\right) + c_1\left(\frac{\partial^2 P_{xx}}{\partial x^2} + 2\frac{\partial^2 P_{xy}}{\partial x \partial y} + \frac{\partial^2 P_{yy}}{\partial y^2}\right) + q$$

$$= I_0\ddot{w}_0 - c_1^2 I_6\left(\frac{\partial^2\ddot{w}_0}{\partial x^2} + \frac{\partial^2\ddot{w}_0}{\partial y^2}\right) + c_1\left[I_3\left(\frac{\partial\ddot{u}_0}{\partial x} + \frac{\partial\ddot{v}_0}{\partial y}\right) + J_4\left(\frac{\partial\ddot{\phi}_x}{\partial x} + \frac{\partial\ddot{\phi}_y}{\partial y}\right)\right],$$

$$\frac{\partial\bar{M}_{xx}}{\partial x} + \frac{\partial\bar{M}_{xy}}{\partial y} - \bar{Q}_x = J_1\ddot{u}_0 + K_2\ddot{\phi}_x - c_1 J_4\frac{\partial\ddot{w}_0}{\partial x},$$

$$\frac{\partial\bar{M}_{xy}}{\partial x} + \frac{\partial\bar{M}_{yy}}{\partial y} - \bar{Q}_y = J_1\ddot{v}_0 + K_2\ddot{\phi}_y - c_1 J_4\frac{\partial\ddot{w}_0}{\partial y}, \tag{2}$$

where N_{ij} are the normal ($i = j$) and shear ($i \neq j$) force resultants, $\bar{M}_{ij}$ are the moment resultants, $\bar{Q}_{ij}$ are the transverse force resultants, q is the distributed load, and

$$\bar{M}_{\alpha\beta} = M_{\alpha\beta} - c_1 P_{\alpha\beta}, \quad \bar{Q}_\alpha = Q_\alpha - c_2 R_\alpha, \tag{3}$$

$$I_i = \sum_{k=1}^{m}\int_{z_k}^{z_{k+1}} \rho^{(k)} z^i \,\mathrm{d}z \quad (i = 0, 1, 2, \ldots, 6), \tag{4}$$

$$J_i = I_i - c_1 I_i + 2, \quad K_2 = I_2 - 2c_1 I_4 + c_1^2 I_6, \quad c_1 = \frac{4}{3h^2}, \quad c_2 = 3c_1, \tag{5}$$

where m is the number of layers, $\rho^{(k)}$ is the mass density of the kth layer, h is the wall thickness, and (P_{xx}, P_{yy}, P_{xy}) and (R_x, R_y) denote the higher order resultants, given, respectively, as

$$\begin{Bmatrix} P_{xx} \\ P_{yy} \\ P_{xy} \end{Bmatrix} = \int_{-h/2}^{h/2} \begin{Bmatrix} \sigma_{xx} \\ \sigma_{yy} \\ \sigma_{xy} \end{Bmatrix} z^3 \,\mathrm{d}z, \quad \begin{Bmatrix} R_x \\ R_y \end{Bmatrix} = \int_{-h/2}^{h/2} \begin{Bmatrix} \sigma_{yz} \\ \sigma_{xz} \end{Bmatrix} z^2 \,\mathrm{d}z. \tag{6}$$

The resultants are related to the strains by the relationships

$$\begin{Bmatrix} \{N\} \\ \{M\} \\ \{P\} \end{Bmatrix} = \begin{pmatrix} [A] & [B] & [C] \\ [B] & [D] & [F] \\ [E] & [F] & [H] \end{pmatrix} \begin{Bmatrix} \{\varepsilon^{(0)}\} \\ \{\varepsilon^{(1)}\} \\ \{\varepsilon^{(3)}\} \end{Bmatrix}, \tag{7}$$

$$\begin{Bmatrix} \{Q\} \\ \{R\} \end{Bmatrix} = \begin{pmatrix} [A] & [D] \\ [D] & [F] \end{pmatrix} \begin{Bmatrix} \{\gamma^{(0)}\} \\ \{\gamma^{(2)}\} \end{Bmatrix}, \tag{8}$$

where $\varepsilon^{(0)}$ are the membrane strains, $\varepsilon^{(1)}$ are the curvatures, $\varepsilon^{(3)}$ are the high order strains, and $\gamma^{(0)}$ and $\gamma^{(2)}$ are the transverse shear strains and their high order terms, respectively. The stiffnesses in Eqs. (7) and (8) are given in terms of the layer stiffnesses $\bar{Q}_{ij}^{(k)}$ of the kth layer and the positions of the top and bottom faces of the kth layer z_{k+1} and z_k as

$$(A_{ij}, B_{ij}, D_{ij}, E_{ij}, F_{ij}, H_{ij}) = \sum_{k=1}^{n}\int_{z_k}^{z_{k+1}} \bar{Q}_{ij}^{(k)}(1, z, z^2, z^3, z^4, z^6)\,\mathrm{d}z, \quad i,j = 1,2,6; \tag{9}$$

$$(A_{ij}, D_{ij}, F_{ij}) = \sum_{k=1}^{n}\int_{z_k}^{z_{k+1}} \bar{Q}_{ij}^{(k)}(1, z^2, z^6)\,\mathrm{d}z, \quad i,j = 4,5. \tag{10}$$

Note that the stiffnesses E_{ij}, F_{ij} and H_{ij} consist of the terms whose orders are higher than cubic of the plate thickness.

2.2. Displacement finite element method

2.2.1. Unfolded plates

The model described by Eq. (2) is named the *displacement finite element method* by Reddy and Phan [17], which requires the use of Lagrange interpolation of $(u_0, v_0, \phi_x, \phi_y)$ and Hermite interpolation of w_0. A non-conforming element for unfolded plates will thus have 7-d.o.f. per node, i.e., u_0, v_0, w_0, $w_{0,x}$, $w_{0,y}$, ϕ_x, and ϕ_y. The generalized displacements can be approximated over an element Ω^e by the expressions

$$u_0(x,y,t) = \sum_{i=1}^{m} u_i^e(t)\psi_i^e(x,y), \quad v_0(x,y,t) = \sum_{i=1}^{m} v_i^e(t)\psi_i^e(x,y),$$
$$w_0(x,y,t) = \sum_{i=1}^{m} \bar{\Delta}_i^e(t)\varphi_i^e(x,y) \tag{11}$$

and

$$\phi_x(x,y,t) = \sum_{i=1}^{m} X_i^e(t)\psi_i^e(x,y), \quad \phi_y(x,y,t) = \sum_{i=1}^{m} Y_i^e(t)\psi_i^e(x,y), \tag{12}$$

where ψ_i^e denote the Lagrange interpolation functions and φ_i^e are the Hermite interpolation functions. For the non-conforming elements, the three nodal values associated with w_0 are written as

$$\bar{\Delta}_1 = w_0, \quad \bar{\Delta}_2 = \frac{\partial w_0}{\partial x}, \quad \bar{\Delta}_3 = \frac{\partial w_0}{\partial y}. \tag{13}$$

These equations can be rewritten in compact form as

$$\sum_{\beta=1}^{5} \sum_{j=1}^{n_\beta} (K_{ij}^{\alpha\beta}\Delta_j^\beta + M_{ij}^{\alpha\beta}\ddot{\Delta}_j^\beta + S_{ij}^{\alpha\beta}\Delta_j^\beta) - F_i^\alpha = 0, \quad i = 1,2,\ldots,n_\alpha, \tag{14}$$

where $\alpha = 1,2,3,4,5$, $n_1 = n_2 = n_4 = n_5 = 4$, and $n_3 = 12$ for non-conforming elements, Δ_j^β denote the nodal values, $K_{ij}^{\alpha\beta}$ are the stiffness coefficients, $M_{ij}^{\alpha\beta}$ are the mass coefficients, and $S_{ij}^{\alpha\beta}$ are the geometric stiffness coefficients, and F_i^α are the external forces, respectively.

2.2.2. Folded plates

It is known that a global stiffness matrix is singular and ill-conditioned because of the null diagonal terms resulting from the drilling d.o.f. ϕ_z in the transformed element stiffness matrix. As a result, it is not possible to obtain the shape function of the drilling d.o.f. induced by transformation. To resolve this problem in a finite element analysis, we could insert an artificial in-plane rotational angle or equivalently rotational stiffness coefficients. In our analysis, we add an 8th drilling d.o.f. to the existing 7-d.o.f. system, as suggested by Lee et al. [10]. The deformations of each element expressed in the local co-ordinates can be transformed into the

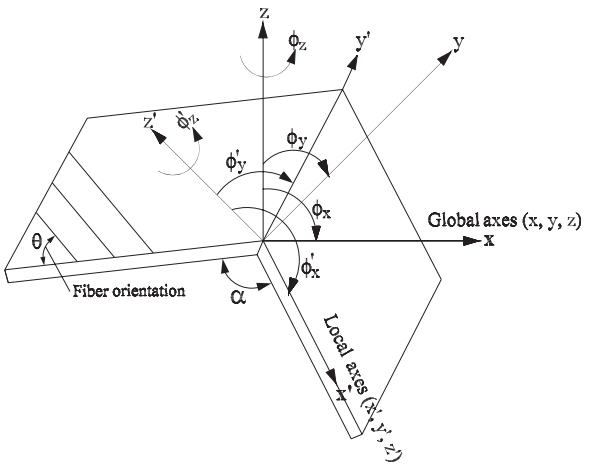

Fig. 2. Coordinate transformation of a folded plate element.

loading co-ordinates using the following transformation relationship (see Fig. 2):

$$\begin{Bmatrix} u_0 \\ v_0 \\ w_0 \\ w_{0,x} \\ w_{0,y} \\ \phi_x \\ \phi_y \\ \phi_z \end{Bmatrix} = \begin{pmatrix} l_{x'x} & l_{x'y} & l_{x'z} & 0 & 0 & 0 & 0 & 0 \\ l_{y'x} & l_{y'y} & l_{y'z} & 0 & 0 & 0 & 0 & 0 \\ l_{z'x} & l_{z'y} & l_{z'z} & 0 & 0 & 0 & 0 & 0 \\ 0 & 0 & 0 & l_{y'y} & -l_{y'x} & 0 & 0 & 0 \\ 0 & 0 & 0 & -l_{x'y} & l_{x'x} & 0 & 0 & 0 \\ 0 & 0 & 0 & 0 & 0 & l_{y'y} & -l_{y'x} & l_{y'z} \\ 0 & 0 & 0 & 0 & 0 & -l_{x'y} & l_{x'x} & -l_{x'z} \\ 0 & 0 & 0 & 0 & 0 & l_{z'y} & -l_{z'x} & l_{z'z} \end{pmatrix} \begin{Bmatrix} u'_0 \\ v'_0 \\ w'_0 \\ w'_{0,x} \\ w'_{0,y} \\ \phi'_x \\ \phi'_y \\ \phi'_z \end{Bmatrix} \tag{15}$$

or, in brief,

$$\{u\} = [T]\{u'\}, \tag{16}$$

where l_{ij} are the direction cosines between the global and local co-ordinates and $[T]$ is the transformation matrix. The primed notations are used to denote the deformations in the local co-ordinates.

The global stiffness matrix is then expressed as

$$[\bar{K}] = [\bar{T}]^{\mathrm{T}}[\bar{K}]'_s[\bar{T}], \tag{17}$$

where

$$[\bar{T}] = \begin{pmatrix} [T] & 0 & 0 & 0 \\ 0 & [T] & 0 & 0 \\ 0 & 0 & [T] & 0 \\ 0 & 0 & 0 & [T] \end{pmatrix}_{32\times 32}, \quad [\bar{K}]'_s = \begin{pmatrix} [K]_{\mathrm{I}} & 0 \\ 0 & [K]_{\mathrm{II}} \end{pmatrix}_{32\times 32}. \tag{18}$$

Note that $[K]_{\mathrm{I}}$ and $[K]_{\mathrm{II}}$ are the real and artificial matrices consisting of 28×28 and 4×4 elements, respectively. Before applying the transformation, the 28×28 matrix is reconstructed into a 32×32 matrix in order to accommodate the drilling d.o.f. ϕ_z for each element. Transformation of the mass matrix is the same as that of the stiffness matrix, that is,

$$[\bar{M}] = [T]^{\mathrm{T}}[\bar{M}]'_S[T]. \tag{19}$$

For a free vibration, the equation of motion is written in the form

$$\{[\bar{M}] - \omega^2[\bar{K}]\} = \{0\}. \tag{20}$$

In order to understand the dynamic behavior of a system, we often need to know only a few low order eigenvalues of the system. In this study, the subspace iteration method [19] is adopted to extract the eigenpairs representing the low order natural frequencies. This method selects a subspace whose dimensions, determined by the desired number of eigenvalues to be obtained, are the same as those of the entire matrix. Then, the Jacobi iteration method is carried out on the selected matrix using the Ritz's base vector as an initial vector. This method has the advantages to effective memory management and computational efficiency as compared to other methods which carry the entire matrix in the computation [19].

3. Numerical results

3.1. Flat and two-folded plates

The finite element formulation described earlier is now implemented to compare the results of our technique with those published by other investigators and also to study the influences of high order terms on the analysis of folded or box composite structures. Fig. 3 shows the dimensions and boundary conditions of a composite box structure analyzed by the aforementioned theories for the materials whose properties are listed in Table 1. Table 2 shows the normalized natural frequencies of an unfolded antisymmetric cross-ply laminate ($[0/90]_n$, $L/h = 5$). The parallel edges on the side of the plate are simply supported while we consider three different boundary conditions for the other two edges of the same plate. As expected, the exact solutions and numerical results obtained from this study are in good agreement with those reported by Reddy [13]. On the other hand, the results obtained using different theories could be noticeably different depending on the given boundary conditions.

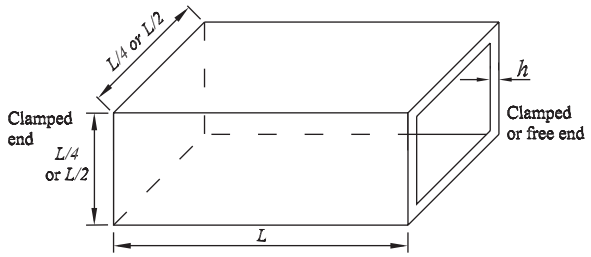

Fig. 3. Dimensions and boundary conditions of a composite box structure analyzed by the HOPT.

Table 1
Mechanical and physical properties of the materials used in this study

Material	Source	E_1	E_2	G_{12}	G_{23}	G_{13}	ν_{12}	ν_{21}	ρ
Material I	[13]	$40E_2$	—	$0.6E_2$	$0.5E_2$	$0.6E_2$	0.25	0.25	—
Material II	[8]	10.92	10.92	4.2	4.2	4.2	0.30	0.30	1000
Material III	[12]	60.70	24.80	12.0	12.0	12.0	0.23	0.23	1300

The units of $E_1, E_2, G_{12}, G_{23}, G_{13}$ are GPa and that of ρ is kg/m^3, respectively. Note that the properties of Material I are normalized by E_2.

Table 2
Normalized frequencies of an unfolded $[0/90]_n$ antisymmetric cross-ply laminate made of Material I

Source	Theory	Solution	Normalized frequency, ω		
			F–S	S–S	C–C
Reddy [13]	HOPT	Exact	6.387	9.087	11.890
		FEM	6.192	9.103	12.053
	FOPT	Exact	6.213	8.833	10.897
		FEM	6.219	8.837	10.906
	CLPT	Exact	7.450	10.721	17.741
		FEM	7.279	11.192	18.694
This study	HOPT	FEM	6.083	9.194	11.972

Letters F, S and C denote free, simply supported, and clamped conditions, respectively. $L/h = 5$, $\omega = \bar{\omega}L^2\sqrt{\rho/E_2}/h$.

Table 3
Normalized values of low order natural frequencies for free vibration of unfolded and folded isotropic plates made of Material II

Folding angle	Mode	Normalized frequency, ω			
α		This study (HOPT)	Niyogi et al. [12] (FOPT)	Liu and Huang [6] (CLPT)	Irie et al. [8] (CLPT)
180°	I	0.0208	0.0200	0.0200	0.0201
(Flat plate)	II	0.0504	0.0489	0.0492	0.0493
	III	0.1272	0.1230	0.1235	0.1234
	IV	0.1605	0.1567	0.1566	0.1577
	V	0.1850	0.1784	0.1787	0.1796
90°	I	0.1211	0.1249	0.1249	—
(Folded plate)	II	0.1348	0.1252	0.1260	—
	III	0.2561	0.2697	0.2579	—
	IV	0.2869	0.2830	0.2892	—
	V	0.3253	0.3266	0.3286	—

$\omega = \bar{\omega}L\sqrt{\rho(1-\nu^2)/E}$.

By contrast, the use of different theories make little differences for isotropic plates regardless of folding conditions. The natural frequencies of unfolded (i.e., flat, $\alpha = 180°$) and two-folded (channel, $\alpha = 90°$) isotropic plates are compared in Table 3. The non-dimensional frequencies of

Table 4
Natural frequencies of two-folded cantilever composite plate (Material III, $L/h = 50$, $\omega = \bar{\omega}L\sqrt{\rho(1-v_{12}^2)/E_1}$)

Angle orientation	Normalized frequency, ω					
	Ref. [12] (FOPT)			This study (HOPT)		
	Mode I	Mode II	Mode III	Mode I	Mode II	Mode III
$[\pm 30]_{ns}$	0.0901	0.0989	0.2035	0.0925	0.1128	0.2057
$[0/90]_{ns}$	0.0896	0.0934	0.2044	0.1055	0.1156	0.1990
$[0/90]_{2n}$	0.0987	0.0993	0.1992	0.0982	0.1068	0.2008
$[45/-45/45]_n$	0.0914	0.1035	0.1988	0.0897	0.1102	0.2068

Table 5
Normalized natural frequencies of cross-ply composite box beams with clamped ends (Material I, $L/h = 10$, $\omega = \bar{\omega}L^2\sqrt{\rho/E_2}/h$)

Mode	Normalized frequency, ω			
	$[0]_n$	$[0/90]_n$	$[0/90/0]_n$	$[0/90]_{2n}$
I	13.884	20.401	17.609	20.918
II	15.130	23.098	18.951	23.419
III	26.870	25.651	25.273	25.891
IV	31.176	42.213	38.817	44.652

the unfolded thin plate analyzed by the HOPT are slightly higher than the others because of the small effects of the high order terms in Eqs. (7) and (8). However, in the case of thick plates ($L/h > 10$), the frequencies obtained by the HOPT show the lowest values because of the significant influences of the high order terms [13]. The complete analysis of these effects is beyond the scope of this paper. For the folded plates, it is observed that both HOPT and FOPT give good results with negligible differences between them. A free vibration analysis of a two-folded cantilever plate made of E-glass/Epoxy composite is carried out for a folding angle $\alpha = 90°$. The length L used in this study is 2.0 m and each fold length of the cantilever is $L/3$. Table 4 shows the three lowest natural frequencies for various layup sequences. Note that a 6×3 mesh of nine-node quadratic elements (FOPT) is used by Niyogi et al. [12], while a 12×6 mesh of non-conforming elements (HOPT) is used in this study. The natural frequencies obtained by the HOPT are mostly higher than those by the FOPT. The differences between the theories depend on many parameters such as ply angles, number of layers, length-to-thickness ratio, and boundary conditions.

3.2. Box beams

Table 5 shows the normalized natural frequencies of cross-ply composite box beams with clamped ends. It can be observed from the table that the frequencies of the $[0/90]_n$ and $[0/90]_{2n}$ composites are higher than those of the $[0]_n$ and $[0/90/0]_n$, and that the difference between those of $[0/90]_n$ and $[0/90]_{2n}$ is negligible. It may also be observed that the natural frequency tends to increase as the number of layers increases. Table 6 shows the normalized natural frequencies of

Table 6
Normalized natural frequencies of angle-ply composite box beams with clamped ends (Material I, $L/h = 10$, $\omega = \bar{\omega}L^2\sqrt{\rho/E_2}/h$)

Mode	Normalized frequency, ω			
	$[\pm 30]_s$	$[\pm 45]_s$	$[\pm 60]_s$	$[\pm 75]_s$
I	27.090	39.776	46.855	35.884
II	29.491	43.120	51.006	40.236
III	38.205	45.694	55.896	47.311
IV	47.081	56.526	59.162	62.427

Table 7
Normalized natural frequencies of clamped box structures for various values of L/h ratio

End condition	Mode	Normalized frequency, ω				
		Length-to-thickness ratio, L/h				
		5	10	20	50	100
Clamped	I	10.258	18.759	33.760	62.053	66.884
		(8.175)	(11.965)	(14.235)	(15.186)	(15.350)
	II	10.821	19.872	36.297	66.674	79.396
		(9.221)	(13.054)	(15.526)	(16.585)	(16.770)
	III	15.985	32.768	55.330	71.352	91.062
		(11.968)	(24.666)	(35.850)	(40.495)	(41.553)
	IV	22.305	44.026	65.249	75.258	95.457
		(17.094)	(27.188)	(38.276)	(41.854)	(42.687)
Cantilever	I	4.699	8.593	16.500	38.969	63.475
		(1.937)	(2.506)	(2.543)	(2.560)	(2.562)
	II	5.076	9.282	17.883	42.349	67.007
		(3.029)	(3.892)	(4.060)	(4.143)	(4.159)
	III	6.414	11.491	22.039	54.257	73.108
		(5.676)	(11.352)	(15.066)	(15.774)	(15.897)
	IV	12.218	21.504	33.379	57.907	75.678
		(9.428)	(13.324)	(17.453)	(18.356)	(18.552)

The number shown in parentheses are the frequencies of unfolded plates (Material I, $[0/90]_s$, $\omega = \bar{\omega}L^2\sqrt{\rho/E_2}/h$).

symmetric angle-ply composite box beams with clamped ends. Note that the frequency in this case is heavily dependent on the fiber orientation. Among these, the frequencies of the $[\pm 60]_s$ composites exhibit the highest values. We may conclude from these results that, in general, the natural frequency of an angle-ply composite box beam is higher than that of a crossply laminate for the same number of layers. Table 7 shows the natural frequencies of clamped and cantilever box beams tabulated as a function of length-to-thickness ratio L/h (square box sections, symmetric cross-ply laminates of $[0/90]_s$, Material I). It is known in general that the natural frequency of a flat composite plate approaches asymptotically a constant value as the length-to-thickness ratio increases, because the transverse shear deformation terms become negligibly small

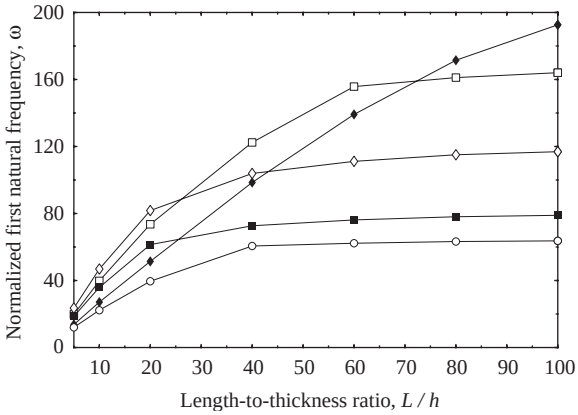

Fig. 4. First order natural frequency of angle-ply composite box beams for various ply angles as a function of length-to-thickness ratio, L/h ($\omega = \bar{\omega}(L^2/h)\sqrt{\rho/E_2}$); ♦, $[\pm 30]_s$; □, $[\pm 45]_s$; ◇, $[\pm 60]_s$; ▩, $[\pm 75]_s$; ○, $[\pm 90]_s$.

for thin laminates [14]. This behavior usually leads us to a conclusion that a simple FOPT is sufficient to analyze unfolded structures. However, Table 7 suggests us that the influence of shear terms may play certain roles in determining the structural behavior of folded or box structures. It is easy to understand that the high order shear terms are signified by the sectional properties, e.g., the moment of inertia, even for the same wall thickness. The numbers shown in parentheses are the frequencies of unfolded plates, in which the values approach a constant as the length-to-thickness ratio increases, especially for high ratios $L/h > 50$. On the other hand, the frequency for the box beam tends to increase sharply in the same range. We may not neglect the shear terms in analyzing folded structures, for the contributions made by the high order terms could be significant. The HOPT is thus used in our analysis to achieve better accuracy. The effects due to the shear terms may be influenced by many factors. One of the most influencing factors is ply orientation. Fig. 4 show the frequency of a box beam for various layup sequences. As shown in the figure, the rate of convergence varies for different conditions. Although it is beyond the scope of this paper, we may pay attention to the fact that the shear terms and their high order terms are dependent on other factors such as the shape and material properties.

Fig. 5 shows the mode shapes of symmetric cross-ply box beams with clamped ends. Each figure represents (a) symmetric vertical bending, (b) symmetric horizontal bending, (c) torsional, and (d) antisymmetric horizontal bending modes, respectively. Also shown in Figs. 6 and 7 are the mode shapes of $[0/90]_s$ and $[\pm 45]_s$ composite cantilever box beams. It is interesting to observe that the cross-sectional shapes are distorted for the $[\pm 45]_s$ angle-ply composite beam as shown in Fig. 7. This is clearly due to the effect of shear coupling. The degree of distortion is determined by the ply angle and the length-to-thickness ratio.

4. Summary and conclusion

A technique based on high order plate theory is developed to analyze the static and free-vibration behavior of folded composite structures. It could be an attractive approach, not only

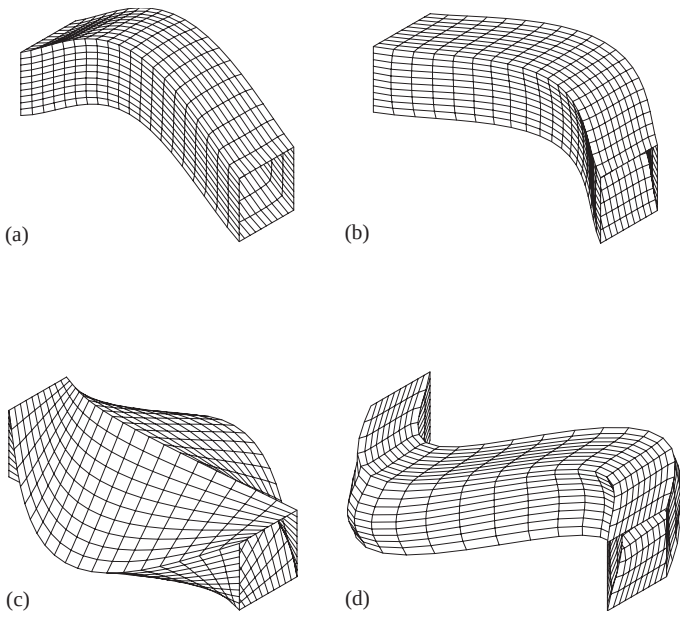

Fig. 5. Mode shapes of the lowest modes for a $[0/90]_s$ cross-ply composite box beam with clamped ends for $L = 20$, $L/h = 10$: (a) Mode I; (b) Mode II; (c) Mode III; (d) Mode IV.

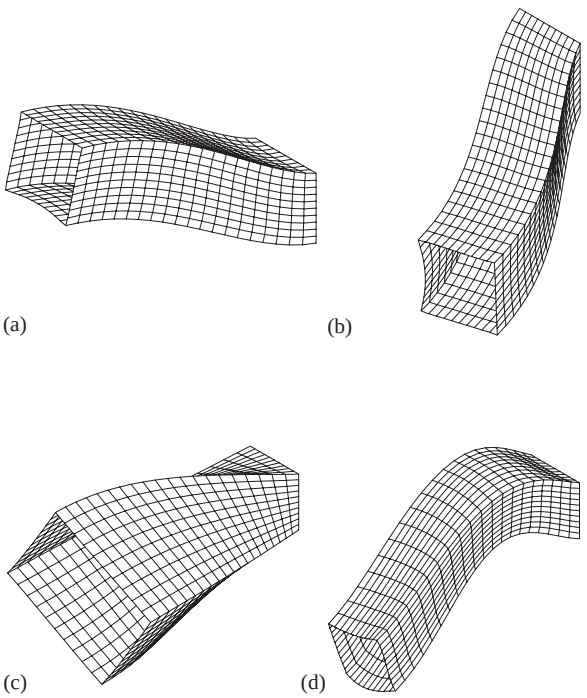

Fig. 6. Mode shapes of the lowest modes for a $[0/90]_s$ cantilever composite box beam for $L = 20$, $L/h = 10$: (a) Mode I; (b) Mode II; (c) Mode III; (d) Mode IV.

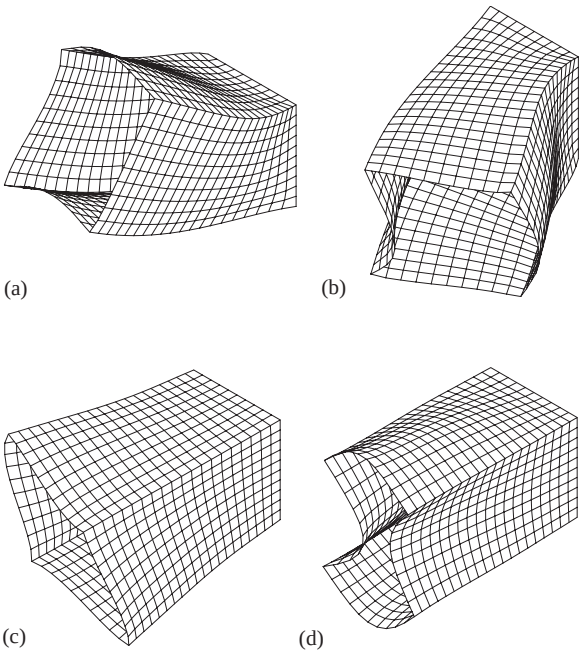

Fig. 7. Mode shapes of the lowest modes for a $[\pm 45]_{ns}$ cantilever composite box beam for $L = 10, L/h = 5$: (a) Mode I; (b) Mode II; (c) Mode III; (d) Mode IV.

because it is computationally efficient and accurate but also because we can avoid assuming shear factors that is mandatory in FOPT. The technique is then implemented for folded and box beam structures of various layup sequences and end conditions to compare the results obtained from different theories (CLPT, FOPT, and HOPT). It is observed that the use of different theories make little difference for isotropic plates regardless of folding conditions, but the difference becomes significant for anisotropic composites, even for unfolded ones, depending on the layup configuration and boundary conditions. For folded composites, e.g., channels or box beams, the significance is even greater, because it is not only the properties of the materials but also the sectional properties of the member that makes large contributions to the overall behavior of the structure. It may be concluded from this study that the effect of transverse shear deformation, largely governing the behavior of thick or folded composite structures, should not be neglected and thus the high order plate theory should be used to analyze such structures for better accuracy.

References

[1] J.E. Goldberg, H.L. Leve, Theory of prismatic folded plate structures, *Journal of the International Association for Bridge and Structural Engineering* 17 (1957) 59–86.

[2] A. De Fries-Skene, A.C. Scordelis, Direct stiffness solution for folded plates, *Journal of the Structural Engineering Division* 90 (1964) 15–47.

[3] A.C. Scordelis, Analysis of simply supported box girder bridges, Structural Engineering and Structural Mechanics Report, SESM 66-17, University of California, Berkeley, 1966.

[4] K.H. Chu, E. Dudnik, Concrete box girder bridges analyzed as folded plates, Concrete Bridge Design, ACI Publications SP-23, MI, 1969.
[5] Y.K. Cheung, Folded plate structures by finite strip method, *Journal of the Structural Engineering Division* 95 (1969) 2963–2979.
[6] W.H. Liu, C.C. Huang, Vibration analysis of folded plates, *Journal of Sound and Vibration* 157 (1992) 123–137.
[7] O.C. Zienkiewicz, R.L. Taylors, *The Finite Element Method Volume II : Solid Mechanics*, Butterworth–Heinemann, Oxford, 2000.
[8] T. Irie, G. Yamada, Y. Kobayashi, Free vibration of a cantilever folded plate, *Journal of the Acoustical Society of America* 76 (1984) 1743–1748.
[9] A.N. Danial, J.F. Doyle, S.A. Rizzi, Dynamic analysis of folded plate structures, *Journal of Vibration and Acoustics* 118 (1996) 591–598.
[10] R.C. Lee, S.Y. Lee, S.S. Yhim, A study on the dynamic responses of PSC box girder bridge under the moving load, *Proceedings First International Conference on Bridge Maintenance Safety and Management*, Barcelona, 2002.
[11] R. Suresh, S.K. Malhotra, Vibration and damping analysis of thin-walled box beams, *Journal of Sound and Vibration* 215 (1998) 201–210.
[12] A.G. Niyogi, M.K. Laha, P.K. Sinha, Finite element vibration analysis of laminated composite folded plate structures, *Journal of Shock and Vibration* 6 (1999) 273–283.
[13] J.N. Reddy, *Mechanics of Laminated Composite Plates: Theory and Analysis*, CRC Press, New York, 1997.
[14] A.A. Khdeir, J.N. Reddy, Analytical solutions of refined plate theories of cross-ply composite laminates, *Journal of Pressure Vessel Technology* 113 (1991) 570–578.
[15] M.A.V. Krishna, Higher order theory for vibration of thick plates, *The American Institute of Aeronautics and Astronautics Journal* 15 (1977) 1823–1824.
[16] A. Bhimaraddi, L.K. Stevens, A high order theory for free vibration of orthotropic, homogeneous and laminated rectangular plates, *Journal of Applied Mechanics* 51 (1984) 195–198.
[17] J.N. Reddy, N.D. Phan, Stability and vibration of isotropic, orthotropic, and laminated plates according to a higher-order shear deformation theory, *Journal of Sound and Vibration* 98 (1985) 157–170.
[18] M.V.V. Murthy, An improved transverse shear deformation theory for laminated anisotropic plates, NASA Technical Paper 1903, 1981, pp. 1–37.
[19] K.J. Bathe, *The Finite Element Procedures in Engineering Analysis*, Prentice-Hall, Englewood Cliffs, NJ, 1996.